Published in final edited form as:
Proc IEEE Int Symp Biomed Imaging. 2009 August 7; 2009: 1075–1078. doi:10.1109/ISBI.2009.5193242.

OPTIMIZATION OF 3-D IMAGE-GUIDED NEAR INFRARED SPECTROSCOPY USING BOUNDARY ELEMENT METHOD

Subhadra Srinivasan, **Colin Carpenter**, **Brian W. Pogue**, and **Keith D. Paulsen**
Thayer School of Engineering, Dartmouth College, Hanover, NH-03755

Abstract

Multimodality imaging systems combining optical techniques with MRI/CT provide high-resolution functional characterization of tissue by imaging molecular and vascular biomarkers. To optimize these hybrid systems for clinical use, faster and automatable algorithms are required for 3-D imaging. Towards this end, a boundary element model was used to incorporate tissue boundaries from MRI/CT into image formation process. This method uses surface rendering to describe light propagation in 3-D using diffusion equation. Parallel computing provided speedup of up to 54% in time of computation. Simulations showed that location of NIRS probe was crucial for quantitatively accurate estimation of tumor response. A change of up to 61% was seen between cycles 1 and 3 in monitoring tissue response to neoadjuvant chemotherapy.

Keywords

near infrared; MRI; 3-D; boundary element method; breast cancer

1. INTRODUCTION

A major focus of on-going studies has been to increase the spatial resolution and create complementary imaging systems by combining different modalities, such as MRI-DOT [1], X Ray-DOT [2], and Ultrasound-DOT [3]. Multimodality imaging systems are emerging as integrative solutions for imaging biophysical, functional as well as structural changes in tissue composition. At Dartmouth College, a combined MRI with near infrared (NIR) imaging system has been developed for diagnosis of breast cancer and treatment monitoring [1]. An alternate system combining CT with fluorescence imaging is also in its final stages, for molecular imaging in small animals. These hybrid systems have bypassed the resolution limit of DOT (3-5 mm) in favor of the sub-millimeter resolution possible from MRI, X-Ray and Ultrasound by utilizing a-priori structural information to guide the DOT image recovery. This approach merges the strengths of structural information provided by a high-resolution modality with the strengths of functional content provided by optical spectroscopy.

These technical developments in imaging systems warrant faster and more accurate algorithms that can intelligently incorporate the anatomical features from MRI/CT into the optical image recovery. Towards this end, a boundary element approach has been developed for 3-D image-guided NIR spectroscopy (IG-NIRS) under the assumptions that the tissue boundaries obtained from MRI/CT are exact and that each tissue type is piece-wise constant [4]. The strength of the BEM lies in easier and more reliable mesh generation schemes since only surface discretization is required. This in turn makes automation possible for processing large clinical data sets. This method can be applied for spectroscopy by solving the diffusion equation; and for fluorescence by solving a set of coupled diffusion equations for excitation and emission wavelengths.

In this work, we have presented results from optimization of this method for clinical use in terms of computational time and guidance for alignment of optical fiber probes. This was used to monitor response of breast tissue in-vivo to neoadjuvant chemotherapy showing that spectroscopy may yield important additional information to MRI for predicting response.

2. METHODS

The diffusion approximation to radiative transport equation was used to model light propagation in tissue. This equation is valid for imaging domains where the scattering dominates over absorption as is the case in the breast tissue in the near infrared wavelength range[5].

Under the assumption that tissue boundaries (interior and exterior) can be obtained from MRI or CT and each tissue type is piecewise constant, the diffusion equation reduces to a modified Helmholtz equation given by:

$$\nabla \boldsymbol{D}_l \nabla \Phi - k_l^2 \Phi = -q_0(r,\omega) \tag{1}$$

where k_l is the wave number, constant in sub-domain l [6,7], and for a particular frequency ω, $k_l^2 = (\mu_a(r) + \frac{i\omega}{c})$.

The fundamental Green's function solution is readily available for this equation and can be used to derive the BEM formulation[8]. The details of this formulation can be found elsewhere [4].

The image reconstruction involves an iterative procedure based on minimization problem given by [9]:

$$\chi^2 = \sum_{j=1}^{M} \left(\Phi_j^{meas} - \Phi_j^{cal} \right)^2 \tag{2}$$

where M is the total number of measurements at each wavelength, and Φ_j^{means} and Φ_j^{cal} are the measured and calculated fluence respectively, at the boundary for each measurement point j. By coupling the measurements obtained at all the wavelengths together and applying spectral relationships defining absorption characteristics of oxyhemoglobin, deoxyhemoglobin and water as well as scattering relationships defined empirically, into the reconstruction, it is possible to obtain the NIRS parameters directly [10]. This use of spectral constraints is known to improve accuracy of recovered spectroscopic parameters and reduce cross-talk [10-12]. We implemented this into the BEM-based reconstruction so that the update in the chromophore concentrations and scatter could be recovered directly. Results from experiments showed that changes in total hemoglobin could be tracked linearly and the hill curve for oxygen saturation could be recovered with a mean error of 6.6%[13]. The BEM reconstructions were found to be faster than FEM for multi-region problems as described earlier[4]. This was applied to recover estimates of breast tissue in-vivo imaged using the hybrid-imaging framework. The details of the instrumentation have been described previously[1]. Briefly, frequency domain measurements of amplitude and phase after transmission through breast tissue were obtained simultaneously with the MRI. The combined data was processed to yield NIRS estimates of total hemoglobin, oxygen saturation, water and scatter in the adipose, fibroglandular and tumor tissues.

3. RESULTS

3.1. Image-segmentation & Surface-rendering

The anatomical structures of interest were obtained from MRI for breast spectroscopy using image segmentation techniques and surface rendering. A commercial software package (MimicsTM, Materialise Inc.) was used for this purpose, which employs thresholding and region-growing techniques. The surface rendering from segmented adipose, fibroglandular and tumor tissues from a subject with cancer is shown in figure 1. This technique works seamlessly with clinical data though sometimes manual editing of the segmented masks may be required for noisy images. This can also be used for segmentation of CT images to recover imaging domain description for fluorescence imaging using BEM. An example of this is shown in Figure 2. These surfaces can be used directly by the BEM toolbox for recover of tissue-specific volumetric estimates.

3.2 Parallel Processing of Image-recovery

The reconstruction for the NIRS parameters benefits from parallelization especially because 3-D computing is time-consuming. This was accomplished using Matlab distributive computing toolbox on a beowoulf cluster comprising of 8 processors per node with shared memory of up to 16 Gigabytes. The time of computation for a single forward model on a patient-specific imaging domain segmented from MRI, is shown in Figure 3.

Using two processors per node showed an improvement of 30% with respect to using a single processor per node. Use of 8 processors improved the time by 54%. Currently, this is the configuration used for clinical studies.

3.3 Alignment of NIR probe with location of cancer

The optical fiber probe positioning will likely affect the resulting reconstructed values in the tissue types especially in the case of cancer. This was found to be true in a clinical study presented earlier. In evaluate the effect of the imaging plane on the recovered tumor values further, a simulation study was undertaken. In this study, a typical breast shape obtained from MRI segmentation was used, with a 32mm tumor simulated in the center of the domain (Figure 4(a)). The red markers show the optical fiber positions. The plane of the fibers was varied systematically in distance separations of 2.5 mm from the center of the tumor to the nipple. Measurements of intensity and phase were simulated for each plane and 1% noise was added. Typical breast concentrations were used for this study. Then error in the reconstructed values for total hemoglobin and water are shown in Figure 4(b). The error in hemoglobin scaled with distance with a slope of 2.3, indicating that there is a 23% error incorporated into the estimation for every 1 cm offset in the probe placement. There is nearly 20% error in water for 1 cm offset in the distance of the imaging plane. This illustrates the importance of aligning the optical probe using image guidance. Further simulations are underway to understand the trend in these estimates.

3.4 Changes in NIRS Parameters during neoadjuvant chemotherapy

The BEM approach was used to reconstruct IG-NIRS estimates of total hemoglobin, oxygen saturation, water and scatter in a subject undergoing neoadjuvant chemotherapy. A 36-year old volunteer was imaged consequtively during the course of treatment through six cycles of TAC. This subject was confirmed by pathology after treatment, to have complete pathological response. The recovered estimates for each tissue type (adipose, fibroglandular and tumor delineated through MRI) were normalized and the overall response was obtained by multiplying the response for each tissue type. This was done to desensitize the measurement to any changes in the optical fiber placement since the background values will be less affected

by changes in the probe distances. The results are shown in Figure 5. There was a 28% change in total hemoglobin in the overall breast between cycles I and II; and 61 % between cycles I and III.

4. CONCLUSIONS

A BEM approach was used to model light propagation in tissue using only surface discretization. This was optimized for clinical use by parallelization in a multi-processing cluster, which provided a 54% improvement in time of computation. The method was used to study the importance of aligning the optical measurement plane to lie in the plane of the tumor. Simulations showed that 23% error is incorporated for a 1cm offset in the plane of the optical measurement. 20% error in water was incorporated for this offset. This method was further used to monitor response to neoadjuvant chemotherapy; results showed a decrease of 28% between cycle I and II; and 61% between cycle I and III indicating that the method may be a useful add-on to MRI for predicting response to therapy. Further clinical studies are underway to evaluate this in a phase I clinical trial.

Acknowledgments

This work was funded through NIH grant R01EB007966.

REFERENCES

1. Carpenter C, Pogue BW, Jiang S, Dehghani H, Wang X, Paulsen KD, Wells WA, Forero J, Kogel C, Weaver J, Poplack SP, Kaufman PA. Image-guided optical spectroscopy provides molecular-specific information in vivo: MRI-guided spectroscopy of breast cancer hemoglobin, water & scatterer Size. Optics Letters 2007;32:933–935. [PubMed: 17375158]
2. Zhang Q, Brukilacchio TJ, Li A, Stott JJ, Chaves T, Hillman E, Wu T, Chorlton M, Rafferty E, Moore RH, Kopans DB, Boas DA. Coregistered tomographic x-ray and optical breast imaging: initial results. J Biomed Opt 2005;10:024033–0240339. [PubMed: 15910106]
3. Zhu Q, Cronin EB, Currier AA, Vine HS, Huang M, Chen N, Xu C. Benign versus malignant breast masses: optical differentiation with US-guided optical imaging reconstruction. Radiology 2005;237:57–66. [PubMed: 16183924]
4. Srinivasan S, Pogue BW, Carpenter C, Yalavarthy PK, Paulsen KD. A boundary element approach for image-guided near-infrared absorption and scatter estimation. Medical Physics 2007;34:4545–57. [PubMed: 18072520]
5. Farrell TJ, Patterson MS, Wilson BC. A diffusion theory model of spatially resolved, steady-state diffuse reflectance for the noninvasive determination of tissue optical properties. Med. Phys 1992;19:879–888. [PubMed: 1518476]
6. Fedele F, Eppstein MJ, Laible JP, Godavarty A, Sevick-Muraca EM. Fluorescence photon migration by the boundary element method. Journal of computational physics 2005;210:109–132.
7. Sikora J, Zacharopoulos A, Douiri A, Schweiger M, Horesh L, Arridge SR, Ripoll J. Diffuse photon propagation in multilayered geometries. Phys Med Biol. 2006
8. Brebbia, CA.; Dominguez, J. Boundary elements: an introductory course.
9. Paulsen KD, Jiang H. Spatially varying optical property reconstruction using a finite element diffusion equation approximation. Med. Phys 1995;22:691–701. [PubMed: 7565358]
10. Srinivasan S, Pogue BW, Jiang S, Dehghani H, Paulsen KD. Spectrally constrained chromophore and scattering NIR tomography provides quantitative and robust reconstruction. Applied Optics 2005;44:1858–69. [PubMed: 15813523]
11. Corlu A, Choe R, Durduran T, Lee K, Schweiger M, Arridge SR, Hillman EM, Yodh AG. Diffuse optical tomography with spectral constraints and wavelength optimization. Appl Opt 2005;44:2082–2093. [PubMed: 15835357]

12. Li A, Zhang Q, Culver JP, Miller EL, Boas DA. Reconstructing chromosphere concentration images directly by continuous-wave diffuse optical tomography. Opt Lett Feb 1;2004 29:256–8. [PubMed: 14759043]

13. Srinivasan, S.; Carpenter, C.; Pogue, BW.; Paulsen, KD. Image-guided near infrared spectroscopy using boundary element method: phantom validation. SPIE 2009 BiOS Biomedical Optics Symposium: Multimodal Biomedical Imaging IV; 2009;

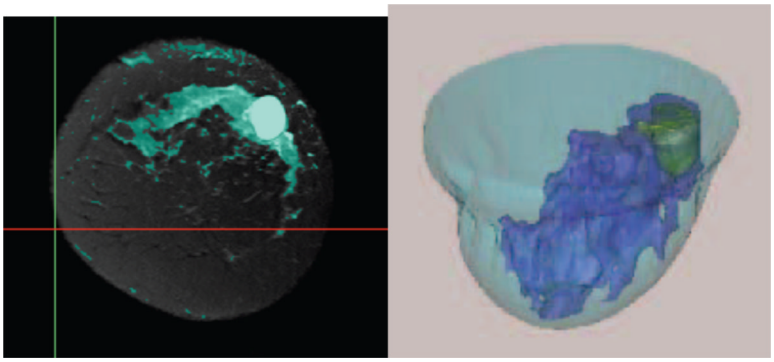

Figure 1.
(a) Example of thresholding of fibro-glandular layer (tagged in turquoise color) from an MR slice is shown. (b) Different surfaces obtained using thresholding: outer surface is shown as transparent, with fibro-glandular tissue in blue as semi-transparent and tumor in yellow as opaque.

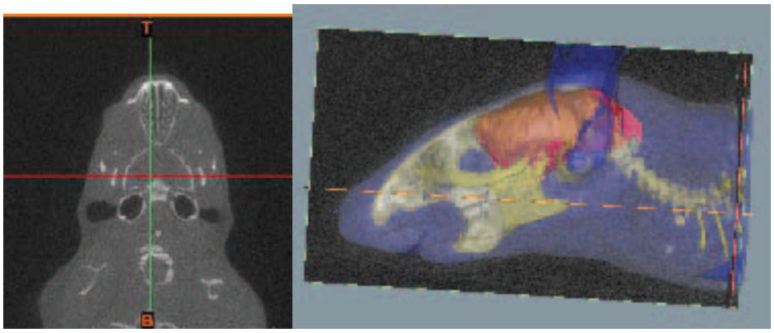

Figure 2.
(a) Cross-section of CT images of a mouse head is shown; (b) The outer surface (blue), bone (yellow) and brain (red) were segmented using Mimics and are shown here.

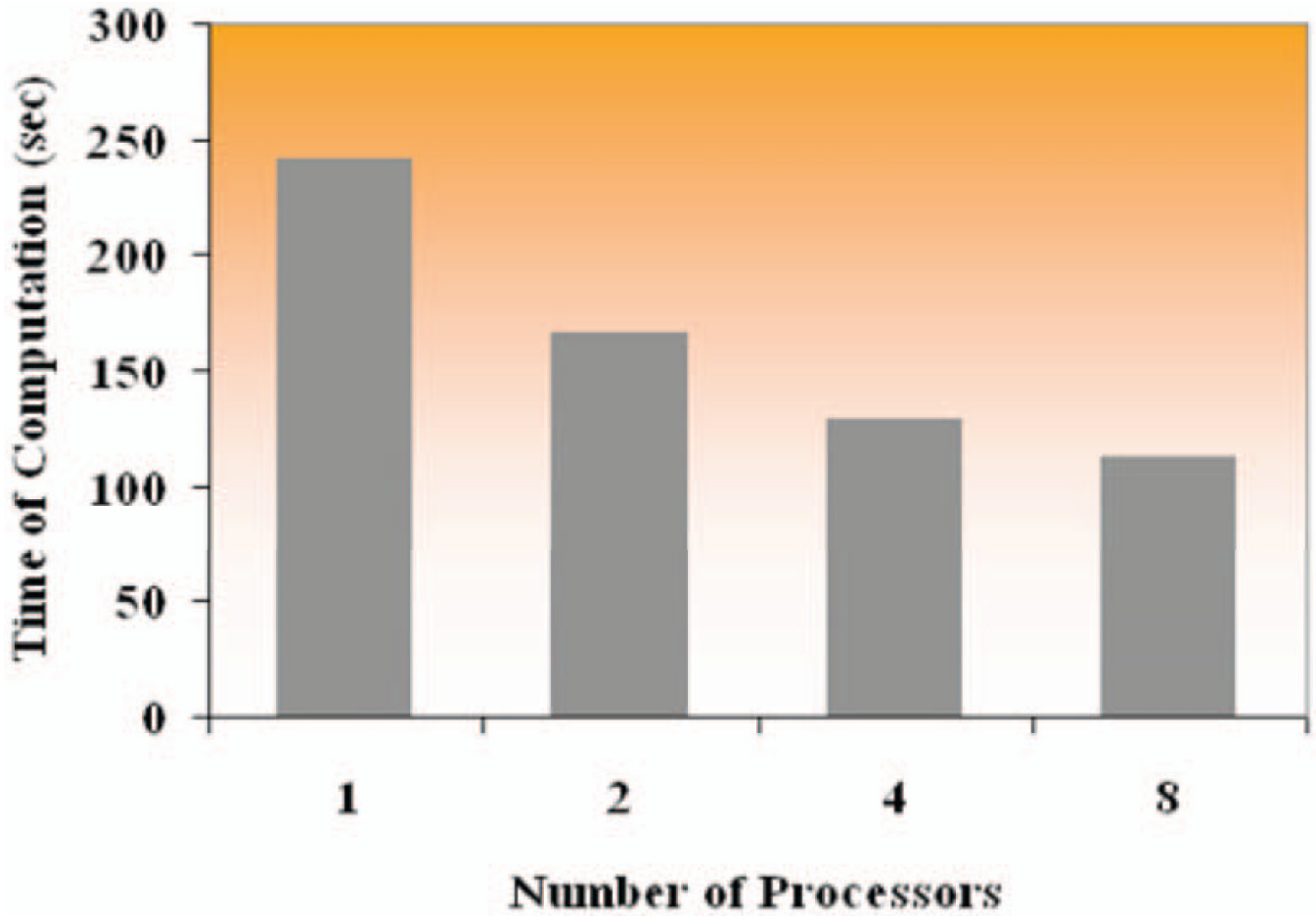

Figure 3.
The time of computation for a forward model solving the diffusion equation on a patient-specific two-region mesh is plotted for varying number of processors. Current configuration uses 8 processors for clinical data analysis, which provides an improvement of 54% in time.

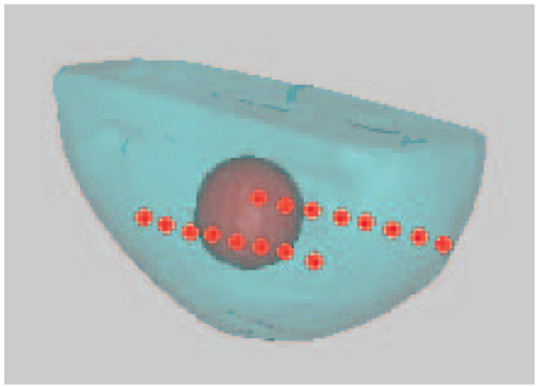

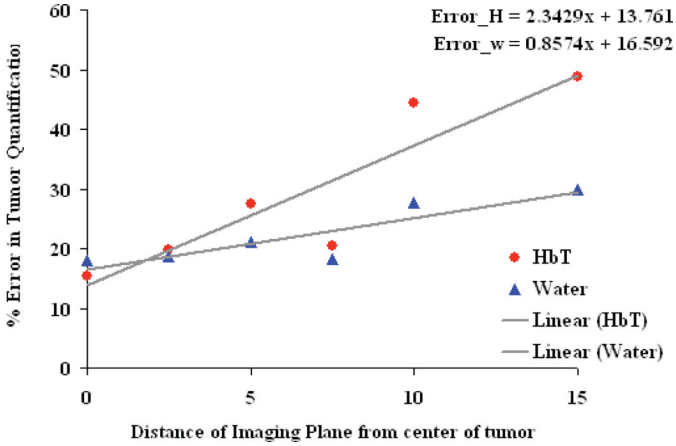

Figure 4.

(a) Segmented breast shape used in simulation study with a simulated 32mm tumor in the center of the domain. Using varying forward and reconstruction meshes and 1% noise in simulated data, the error in the recovered values for total hemoglobin and water are shown in (b) for varying distance of imaging plane (in mm).

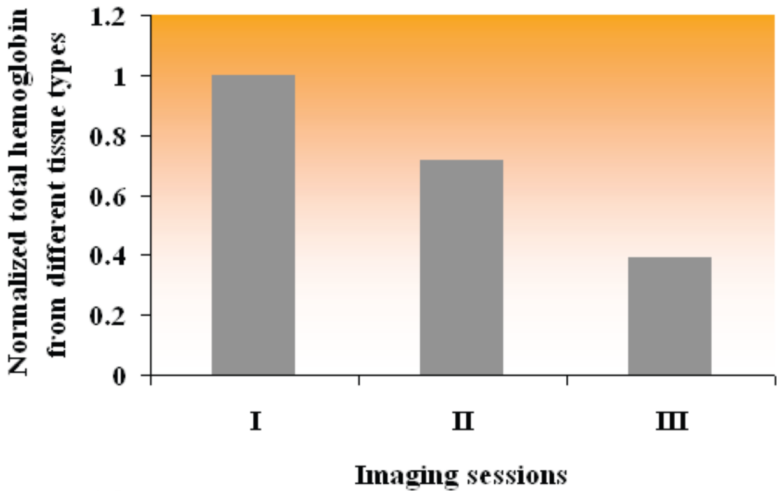

Figure 5.
Changes in total hemoglobin during the course of neoadjuvant chemotherapy.